JOSH
JOURNAL OF SPATIAL HYDROLOGY

Journal of Spatial Hydrology
Vol.12, No.1 Fall 2014

Stomatal Conductance, Canopy Temperature, and Leaf Area Index Estimation Using Remote Sensing and OBIA techniques

S. Panda[1], D.M. Amatya[2], and G. Hoogenboom[3]

Abstract: Remotely sensed images including LANDSAT, SPOT, NAIP orthoimagery, and LiDAR and relevant processing tools can be used to predict plant stomatal conductance (g_s), leaf area index (LAI), and canopy temperature, vegetation density, albedo, and soil moisture using vegetation indices like normalized difference vegetation index (NDVI) or soil adjusted vegetation index (SAVI) developed with near infrared (NIR) and red bands. In this study, we present results of those analyses for two study sites with different plant species: 1) a managed loblolly pine (*Pinus taeda* L.) forest in coastal North Carolina for canopy temperature and g_s and 2) a managed Blueberry (*Vaccinium corymbosum*) orchard within a natural forest in coastal Georgia (Z-Blu orchard) for the LAI. An Object Based Image Analysis (OBIA) technique was employed on the Z-Blu orchard to distinguish the forest species and establish their correlation with LAI using ground-truthing. Similarly, we used OBIA technique for the forest speciation on Turkey Creek watershed at Francis Marion National Forest site in coastal South Carolina with ground-truthing. Both classified images yielded 80% classification accuracy based on field verifications. Similarly, >90% correlation was obtained for the LAI map developed for Z-Blu orchard site plant speciation. However, for the NC pine site, the correlations were poor, with R^2 values of 0.33 and 0.26 for g_s v/s Landsat Middle Infrared (MIR) and g_s v/s Landsat Thermal Infrared TIR models, respectively. This study on advanced image processing approach for forest speciation and ET parameters prediction/estimation can be a basis for similar other studies in the region.

Keywords: ET, NDVI, SAVI, OBIA-segmentation, loblolly pine, blueberry

[1] Associate Professor Institute of Environmental Spatial Analysis, University of North Georgia, 3820 Mundy Mill Road, Oakwood, GA 30566
[2] Research Hydrologist, Center for Forested Wetlands Research, USDA Forest Service, 3734 Highway 402, Cordesville, SC 29434
[3] Director, AgWeatherNet and Professor of Agrometeorology, Washington State University, 24106 North Bunn Road, Prosser, Washington 99350-8694, USA

INTRODUCTION

Plant evaporation and transpiration or evapotranspiration (ET) rate depends upon air and canopy temperature, solar radiation, vapor pressure, wind velocity, and nature and type of the evaporating surface (Viesmann and Lewis, 2004). While plant evaporation occurs mostly from the above canopy interception and understory/litter evaporation, transpiration involves the withdrawal and transport of water from soil/aquifer system from plant roots and stem, and eventually from plant leaves into the atmosphere (Senay et al., 2013). Available heat energy (radiation and air temperature), capacity to transport vapor away from the evaporative surface by wind and humidity, soil water content availability are the guiding factors for the evapotranspiration (Viesmann and Lewis, 2004). Most important parameters that govern ET are leaf area index (LAI), canopy temperature (T_c), stomatal conductance (g_s), wind velocity, and soil moisture or volumetric water content (Panda et al., 2012). Evaporation from canopy interception also depends upon canopy storage capacity and canopy closure/density besides the LAI (Amatya et al., 1996). The LAI is a seasonal parameter and is an indicator of crop growth, for that matter ET as it correlates very well with it (Sun et al., 2011). LAI is also an indication of the biophysical capacity for energy acquisition by the vegetation canopy (Fisher et al., 2008) besides being a key parameter of ecosystem structure (Sun et al., 2011) and a valuable driver in the scaling effort as it is well correlated with normalized difference vegetation index (NDVI) derived from remote sensing images (Hwang et al., 2009). Optical direct method using LI-COR LAI-2200 (LI-COR^{TM}) or hemispherical photographs and semi-direct methods using litter collection and allometric methods are used for local estimation of LAI (Brauman et al., 2012; Sampson et al., 2011; le Maire et al., 2006). Local measurement of plant stomatal conductance is conducted with a direct optical measurement using SC-1 Leaf Porometer (Decagon Devices, Inc.) (Brauman et al., 2012) or using a semi-direct method of vapor pressure deficit algorithm (Pearcy et al., 1989; Sack and Scoffoni, 2012). Stomatal conductance of pine needles was measured by a LiCOR-1600 porometer for estimating and modeling transpiration of pine forests (McCarthy et al., 1991; Amatya et al., 1996; Amatya and Skaggs, 2001). Canopy temperature is estimated with direct measurement using thermometers (Bastiaanssen et al., 1998). However, routine in-situ measurement of these plant parameters are very time consuming and expensive (Panda et al., 2011; Panda et al., 2012; Amatya et al., 2011; Sampson et al., 2011;). Recent studies show the efficiency of remotely sensed data

in estimating stomatal conductance, canopy temperature, LAI and ET (Rouse et al., 1973; Curran, 1980; Moran et al., 1994; Carter, 1998; Justice et al., 1998; Olioso et al., 1999; North, 2002; Provoost et al., 2005; le Maire et al., 2006; Panda et al, 2011; Nouri et al., 2012; and Amatya et al., 2011; Hafeez et al., 2002; Senay et al., 2013).

Remotely sensed images including LANDSAT, SPOT, NAIP orthoimagery can help predict plant stomatal conductance, surface temperature, vegetation stress, and soil moisture amount (Senay et al., 2013; Hafeez et al., 2002; Lllesand and Keifer, 1994). Vegetation indices like normalized difference vegetation index (NDVI) or soil adjusted vegetation index (SAVI) developed with near infrared (NIR) and red are able to remotely determine such forest hydrologic parameters including LAI (Senay et al., 2013; Narasimhan et al., 2003; Lllesand and Keifer, 1994). Remote estimation of LAI is typically conducted using selected individual band spectral reflectance or digital number (DN) values or a combination of them with the development of spectral indices like Normalized Difference Vegetation Index (NDVI) or soil adjusted vegetation indices (SAVI) (Goel and Qin, 1994; Turner et al., 1999; Schultz and Engman, 2000; Coonrod and McDonnell, 2000; Walthall et al., 2004; Willaert et al., 2005; Panda et al., 2011; Panda et al., 2012; Amatya et al., 2011). Remote measurement of stomatal conductance is conducted using suitable band (mid-infrared) of landsat satellite imagery (Lee, 1994; Carter, 1998; Amatya et al., 2011). Thermal band of landsat satellite imagery is used for the remote estimation of canopy temperature (Lee, 1994; Amatya et al., 2011; Senay et al., 2013). Review article by Wang and Qu (2009) explains how numerous studies have already been conducted on remote estimation of soil volumetric water content estimation using satellite, aerial, or simple digital photographic image analysis. However, the secret to the success of the remote application of the ET parameters estimation lies with accurate image segmentation. Advanced image segmentation techniques help distinguish different type of plants among the forest vegetation and thus support accurate remote estimation of these. The processes include analysis of the spectral, textural, and other thematic attributes of the land-use types in the remotely sensed imageries. The latest advanced image processing approach, object based image analysis (OBIA) is the best approach for such classification (Burnett et al., 2003).

Image classification generally comprises four steps including preprocessing, training, decision making, and accuracy assessment (Seetha et al., 2014). The initial step of pre-processing involves

geometric and atmospheric correction, band separation, noise suppression, texture mapping, if necessary, principal component analysis and vegetation index development. The training step includes supervised or unsupervised classification algorithm usage and in this study we used even better OBIA algorithms. This includes the selection of a particular feature in the image that best describes the pattern. The decision step includes choosing the suitable algorithms for comparing the image patterns with the target patterns or finding image patterns that correspond to the field situation. With OBIA, in this step, the clusters are found not only through spectral pattern, but with textural and other thematic attributes as described in earlier paragraph. The final step is to assess the accuracy of the image classification by ground truthing (Seetha, et al., 2014). The most important step of image classification is the selection of the efficient image segmentation or classification algorithm to classify the image with the best accuracy; in this case the advanced OBIA algorithm is tested for our study.

A long-term (1988-2008) monitoring and modeling study to evaluate water balance including ecosystem ET during a life cycle of a managed pine stand, including effects of silvicultural and water management treatments, was just completed using three 25 ha experimental watersheds in eastern North Carolina (NC) (Amatya and Skaggs, 2011; Tian et al., 2012). This study was conducted as a potential basis to the alternative method of estimating ET from different forest species including loblolly pine (*Pinus taeda* L.), pine understory, switchgrass (*Panicum verbatim*), a cellulosic crop with a potential for bioenergy, and its understory intercropping between the pine rows in an ongoing multicollaborative project assessing the hydrologic and water quality effects of switchgrass intercropping in managed pine forests (Ssegane et al., 2014).

The objectives of this study are to:

1. Develop and present a new remote sensing-based procedure for estimating plant canopy temperature, stomatal conductance, and LAI for various forest/vegetation species.
2. Develop an OBIA procedure to segment the study area images with the aid of LiDAR (Light Detection and Ranging) data to classify different plant species in three study areas with dissimilar forest types.

METHODOLOGY

Study Sites

The first study site (Fig. 1a) is on Carteret 7 tract, located in Carteret County, North Carolina (Latitude of 34.822^{o}N and Longitude of -76.668^{o}W), owned and managed by Weyerhaeuser Company. The site consists of three artificially drained experimental watersheds (D1, D2, and D3) that are about 24.7, 23.6, and 26.8 ha in size, respectively. When the watersheds were established in early 1988 the land cover consisted of 14-year old mid-rotation loblolly pine (*Pinus taeda L*.).

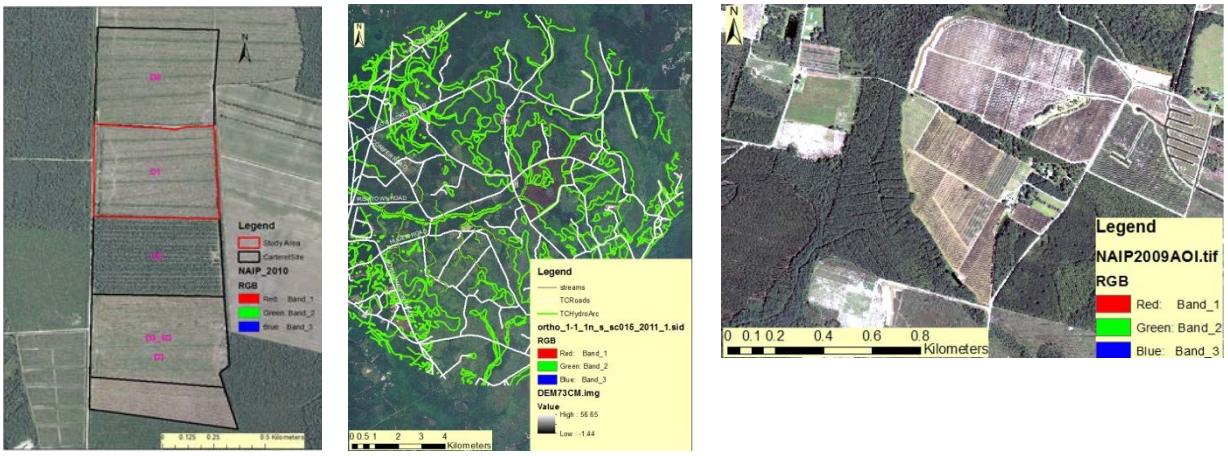

1(a) (AOI 1) 1(b) (AOI 2) 1(c) (AOI 3)

Figure 1: Study area map showing the National Agriculture Imagery Program imagery for North Carolina (NC) site (a.AOI1), South Carolina (SC) site (AOI2), and Georgia (GA) site (b. AOI2).

(Note: From here onwards, the three sites will be described as AOI1, AOI2, and AOI3.)

In 2009, when a new study began to examine effects of switchgrass intercropping in the traditional pine forest AOI1,the then control watershed D1 was harvested and a switchgrass intercropping treatment between beds of young pine was installed in 2012. Similarly, the 2nd watershed (D2) harvested in 1995 and planted in 1997 now served as a control (Ssegane et al., 2014). A switchgrass treatment was installed on the third watershed (D3) that was fully harvested by spring 2010. A fourth treatment watershed (D0) was established north of D1 (Figure 1) in 2009 where a young pine with natural understory treatment was installed for the switchgrass intercropping study. The artificially

bounded watersheds are surrounded by forested land in the north, south, and west, and by agricultural land in the east. McCarthy et al. (1991) characterized the topography of the site as flat Coastal Plain with a gradient of 0.1 % and ground surface at about 3 m above sea level. The Deloss fine sandy loam soil on the site is classified as very poorly drained with a shallow water table under natural conditions. Each watershed is drained by four parallel lateral ditches about 1.4 – 1.8 m deep, spaced 100 m apart (Figure 1). The mean annual rainfall over a 21-year period is 1517 mm with a 10 – 15 % annual increase due to hurricanes and tropical storms (Amatya and Skaggs, 2011). The estimated annual Penman-Monteith based potential evapotranspiration (P-M PET) for a standard grass reference varied between 785 mm to 1254 mm (Amatya and Skaggs, 2011), with an average of 1010 mm for the 21-year (1988-2008) period. For a detailed description of the site soil parameters, climatological data, and forest stands, the readers are referred to McCarthy et al. (1991), Amatya et al. (1996), Amatya and Skaggs (2011), and Ssegane et al. (2014).

The second site, AOI2 is a part of Turkey Creek watershed located adjacent to US Forest Service Santee Experimental Forest at Francis Marion National Forest in coastal South Carolina (Figure 1b-AOI2). This watershed is a third-order stream system draining an area of approximately 5,240 ha (Amatya et al., 2013) and located about 60 km northwest of Charleston near Huger, in Berkeley County, South Carolina (33° 8' N, 79° 48' W). The main channel has braided in some locations, which is anastomosed and stable with mature root systems of bottomland species such as bald cypress and tupelo gum along the streambanks and in some locations in the channel (Amatya and Jha, 2011). Land use within the watershed is comprised of 44% pine forest, mostly loblolly (*Pinus taeda* L.) and longleaf (*Pinus palustris*) pine, 35% thinned forest, 10% forested wetlands, 8% mixed forest, and 3% agricultural, roads, open areas, orchards for sapling development, and impervious areas (Haley, 2007). Sand is the dominate substrate material. The watershed is dominated by poorly drained clayey, mixed soils of the Wahee series mostly on the northern part and Lenoir series, with shallow argillic horizons with less than 3 m depth mostly on the southern part (Amatya and Jha, 2011).

The third study site, AOI3 is in Nahunta, GA (Fig 1 (c) – AOI3). The site is a 52.6 ha (130 acre) well managed commercial blueberry orchard known as ZBlue Berry Farm. The WGS coordinate of the site's location is 31^0 12' 13.95" N and 81^0 58' 50.62". The orchard has different land-uses such as pine

outer cover, two types of blueberry, rabbit eye and high bush, grass, bare soil, waterbodies (pond for irrigation), etc. The site is monitored by a weather station set up by Automated Environmental Monitoring Network (AEMN, www.Georgiaweather.net). Weather or climate parameters including the soil moisture amount is monitored at the weather station. The plant/vegetation species is different here from the study site 1 and, hence, chosen for a contrasting analysis of the OBIA image segmentation technique.

Data Acquisition

The field stomatal conductance for the pine needles measured using a LiCOR-1600 porometer on pine forest stands at the AOI1 site from 1988 to 1992 for estimating transpiration together with the measured LAI and weather parameters both in the field water balance (Amatya et al., 1996; McCarthy et al., 1991) and hydrologic modeling (Amatya and Skaggs, 2001) were used in this study. The data is presented in Table 1 below. The measurements were done on specific tree needles within three experimental plots on a 2-3 week basis. Details of the measurement and analysis procedures are given elsewhere (Amatya et al. 1996; Amatya 1993).

Following Landsat ETM+ 7-band satellite imageries were acquired for the study sites AOI1. The imageries were collected between 1988 and 1992 corresponding to the field stomatal conductance and canopy temperature data measurements acquired during that period.

Table 1. Stomatal Conductance v/s MIR (Middle Infrared) and TIR (Thermal Infrared) data (1988-92)

Month/Year	Julian Day	Stomatal Conductance (mmoles/m^2/s)	MIR band	TIR band	Image Date
Oct-88	287	34.39	47	128	9/16/1988
Oct-88	301	38.77	78	42	10/18/1988
Apr-89	107	46.89	68	114	4/12/1989
May-90	129	39.96	91.45	105.5	5/1/1990
Oct-90	305	35.44	40.88	99	11/25/1990
Feb-91	36	30.81	57.95	112	3/1/1991

Freely downloadable, three-band (RGB) 1m resolution and four-band (RGB & NIR) NAIP (National Agricultural Imagery Program) Imagery of 2011 were acquired for AOI 2 and AOI3 sites, respectively. LiDAR data (30 cm resolution) was obtained for the AOI 2 site along with stream and road network to support OBIA based image classification. For OBIA classification, these geospatial features provided spectral, textural, and thematic attributes of the land-use types supported in OBIA rule sets (described later) development for better image segmentation accuracy. The forest cover classification map for AOI 2 (Figure 2a) site and Z-blu orchard management specification vector (Figure 2b) for AOI 3 were acquired for image classification ground truthing. IDRISI Taiga (*Clark Labs, Clark University, Worcester, MA*) software for high-end image processing and eCognition (*Trimble Geospatial, Westminster, CO*) Developer software for OBIA analysis, QT Modeler (Applied Imagery, Silver Spring, MD) software for LiDAR data processing, and ArcGIS 10 (ESRI, Redlands, CA) software for all spatial data analysis were used in the study.

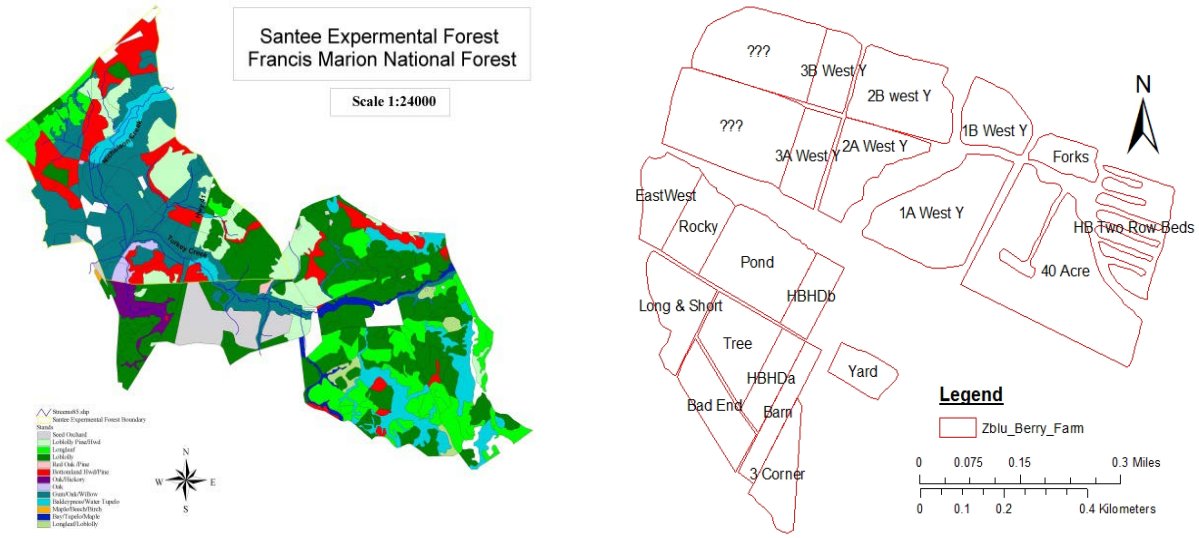

(a) (b)

Figure 2: (a) forest cover classification map for AOI 2 and (b) Z-Blu orchard management vector showing different land-uses (*Courtesy, Witherbee Ranger Station, Francis Marion National Forest, Cordesville, SC and Z-Blue Farm Manager, Nahunta, GA)*.

Individual bands used for the stomatal conductance and plant canopy temperature models for AOI1 were extracted from the Landsat ETM+ imageries in ArcCatalog. Examples of a single date image bands are shown in Figure 3a, b, c, and d.

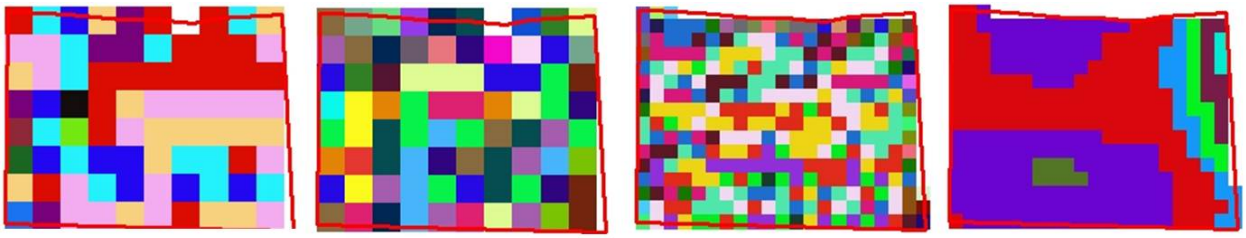

Figure 3: Example of different Landsat band images of AOI 1a in Figure 1 used for estimating stomatal conductance and canopy temperature (NIR – Near infrared, MIR- Middle infrared, and TIR – Thermal infrared)

Image Analysis

Plant canopy temperature, stomatal conductance, and LAI model development

As described earlier, remotely sensed information based stomatal conductance and canopy temperature estimation models were developed for the AOI1 site and LAI estimation model was created for AOI3 site. Thermal (plant canopy temperature) raster was created in IDRISI Tiaga software using the TIR band and the emissivity value of 0.95 (Lillesand and Keifer, 1994) following the equations below:.

$$L_\lambda = \text{offset} + \text{gain} \times DN \qquad \text{Equation (1)}$$

$$T_B = K2 / (\ln((K_1 / L_\lambda) + 1) \qquad \text{Equation (2)}$$

where, offset and gain, K_1, K_2 are user defined parameters, respectively. DN is the digital number in the thermal energy, and T_B is the Blackbody temperature. The constant K_1 must be in $Wm^{-2}\ sr^{-1}\ \mu m^{-1}$ (watts per sq. m. per steradian per micron) and constant K_2 in Kelvin.

$$S_t = TB / (1 + (\lambda \times T_B / \rho) \times \ln \varepsilon \qquad \text{Equation (3)}$$

where, λ = wavelength of emitted radiance in micrometers, $\rho = h \times (c / \sigma) = 1.438 \times 10^{-2}$ (mK), σ is the Boltzmann constant (1.38×10^{-23} J/K), h is the Plank's constant (6.626×10^{-34} Js, c is the velocity of light (2.998×10^{8} m/s), and ε is the emissivity in the range of 0 and 1.Once, the statistics (mean digital) values

of MIR & TIR bands were calculated, they were data logged to the corresponding stomatal conductance values. Multiple regression models were developed with stomatal conductance v/s MIR, and stomatal conductance v/s TIR band digital information in MiniTab 16 (Minitab Inc., State College, PA) statistical software.

LAI raster was developed for the AOI3 site using the relationship developed by Schultz and Engman (2000),

LAI = - ln (SAVI + .371)/.48 (Equation 4),

which calculates LAI using the soil adjusted vegetation index (SAVI) from NAIP orthoimagery.

Forest speciation to support ET based model parameter estimation model development

Finally, forest plant speciation analysis was conducted using the OBIA multiresolution segmentation technique for AOI 2 & AOI 3 sites as ground truth supporting information (Figures 2a and 2bb) was available for both sites to conduct classification accuracy assessment. The AOI1 site did not have any supporting data for accuracy assessment in 1989-1992. With the OBIA image segmentation, image indices, site elevation raster developed with LiDAR, other land-use specifying vector data (mentioned earlier) were used for rule sets development and subsequent multiresolution segmentation.

Individual bands (Red, Green, Blue, and NIR) were separated from the NAIP imageries using ArcCatalog module of ArcGIS10. Vegetation indices, such as NDVI, Green vegetation index (GVI), Soil Adjusted Vegetation Index (SAVI), and Band ratios (BG/NIR^2, RG/NIR^2, and BR/NIR^2) were developed in IDRISI Taiga using Image Calculator and with the below equations

$$NDVI = (\rho_{ir} - \rho_r) / (\rho_{ir} - \rho_r) \quad \text{Equation (5)}$$

$$GVI = (\rho_{ir} - \rho_g) / (\rho_{ir} - \rho_g) \quad \text{Equation (6)}$$

$$SAVI = \left[\frac{(\rho_{ir} - \rho_r)}{(\rho_{ir} + \rho_r + L)}\right] x\,(1+L) \quad \text{Equation (7)}$$

where, ρ_r , ρ_g and ρ_{ir} are spectral reflectance from the R-, G- and NIR-band images, respectively, and the L is a constant that represents the vegetation density. Huete (1988) defined the optimal adjustment factor of L = 0.25 to be considered for higher vegetation density in the field, L = 0.5 for intermediate vegetation density, and L = 1 for the low vegetation density.

LiDAR data was processed for AOI 2 and AOI 3 sites to produce ground elevation raster (DEM) and the plant height raster (nDSM) using the QT Model Builder software. These raster were imported to eCognition software. It was found that NDVI, BG/NIR^2 ratio and Blue band raster were a good representation of spectral behavior of different forest plant species present in both the study areas (AOI 2 and AOI 3). Initial rule sets were developed using spectral characteristics to classify different forest species. Second rule set was developed using plant height raster to distinguish plant species with similar spectral characteristics. (Note: *This rule set was only used with AOI 3*). Because rule sets are site specific to support image classification based on forest species and other land- uses present. Then, the OBIA based shape geometry (Length/width; asymmetry; and compactness) was used to develop the third rule set to distinguish plant species not separated with last two rule sets. Finally, a rule set was developed with proximity to thematic features like roads and streams as particular type of plants grows close to them. (Note: *This rule set was only used with AOI 2*). Ultimately the Multiresolution segmentation procedure was completed with eCognition software using the rule sets. Classification rasters for both the sites were compared with the classification maps (Figures 2a and 2b) obtained from the corresponding land management agencies in those two study areas and classification accuracy assessment was conducted.

Results & Discussion

Plant canopy temperature raster & stomatal conductance models for AOI 1

Figures 4 and 5 represent the correlation models fitted with a second order polynomial for each of the MIR and TIR band DN values, respectively, and the corresponding field measured stomatal conductance values for only six different measurement periods. The computed coefficient of determination (R^2) values obtained with limited field observations (n = 6) for stomatal conductance v/s MIR and stomatal conductance v/s TIR are 0.33 and 0.26, respectively, suggesting a fair relationship between Landsat image band width-based digital values and stomatal conductance for pine trees. We hypothesize that the relationships could possibly be improved with inclusion of more measurements. Figure 6 shows the plant canopy temperature or Thermal raster obtained using equations 1 -3 provided in the Materials & Methods section. The data range in Figure 5 suggests that it is feasible to use the Thermal band raster in such analysis.

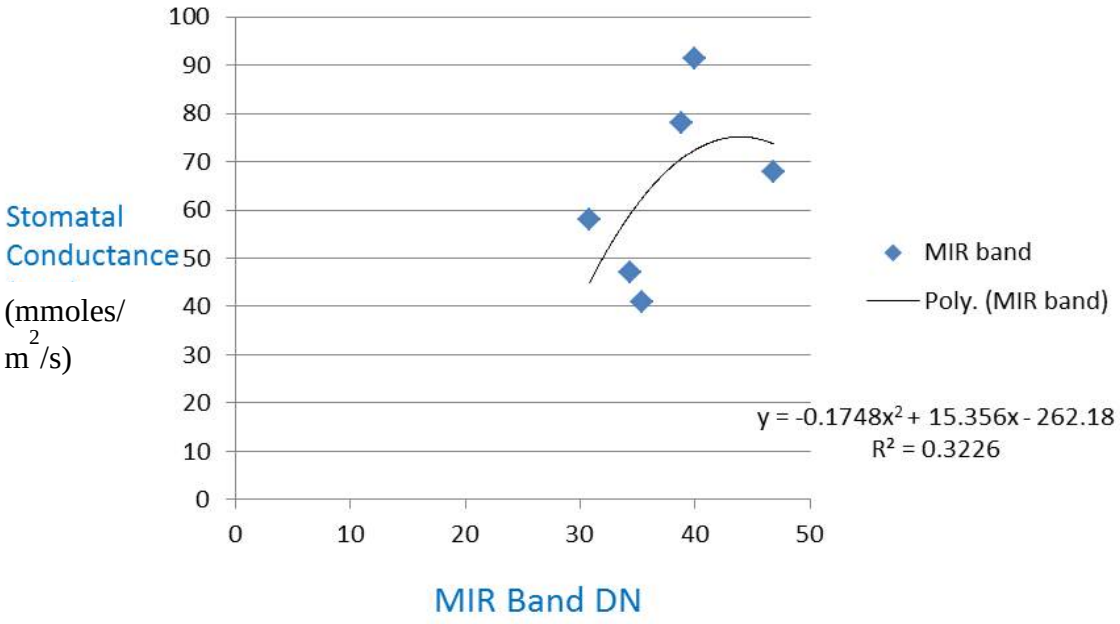

Figure 4: Second order polynomial fitted for s stomatal conductance versus MIR correlational model (n = 6)

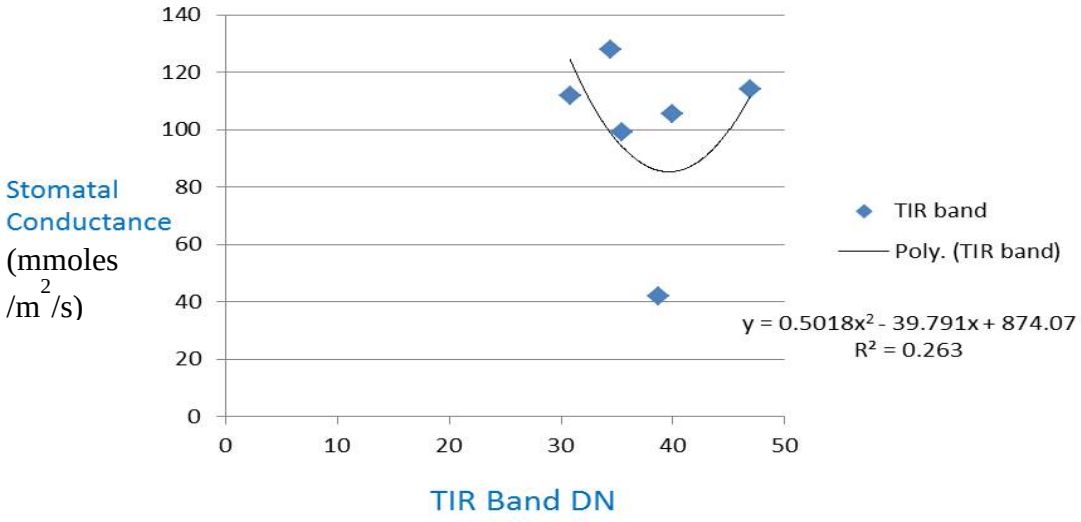

Figure 5: Second order polynomial fitted for a stomatal conductance versus TIR correlational model (n = 6)

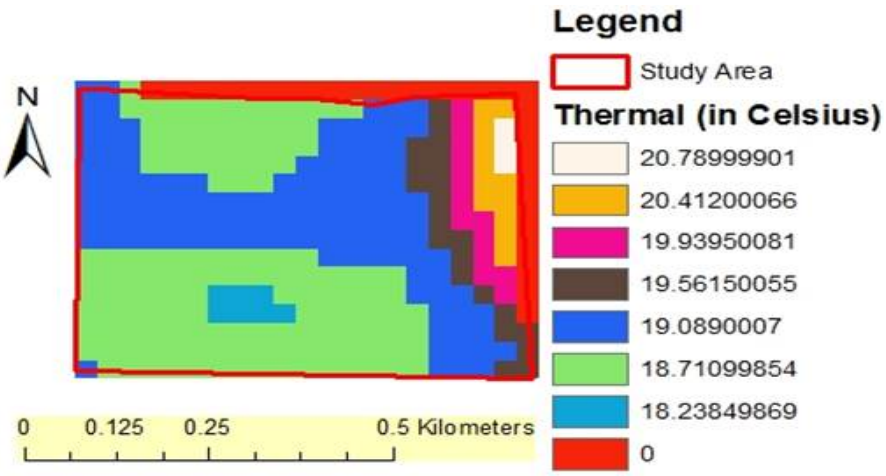

Figure 6: Thermal raster using 06/28/1988 satellite image that shows the surface temperature of pine trees.

Leaf Area Index (LAI) model development for AOI 3 (Z-Blu orchard)

Figures 7 and 8 show the calculated SAVI and LAI rasters for the Z-Blu blueberry orchard (AOI 3) at the GA site developed in IDRISI Taiga software using the 1-m resolution NAIP imagery with equations suggested in the Materials and Methods section. Based on the analysis of the LAI raster for AOI 3data, it is clearly evident that the individual plant species have very specific LAI. With selected locations, the plant/land use types (numbered with integers) when correlated with five different ranges of LAI values (the five groups generated with Jenks classification algorithm supporting five distinct forest species and other land uses in the orchard), coefficient of determination (R^2) values of 0.91 was obtained. The dark green areas in the LAI images indicate various stages of blueberries. Even the different stages of blueberries (new plant rabbit eye (dark green) and older high bush and rabbit eye (faint green) have distinguishable LAIs. The surrounding pine and oak forest species have completely distinguishable LAI values as obtained by the modeling.

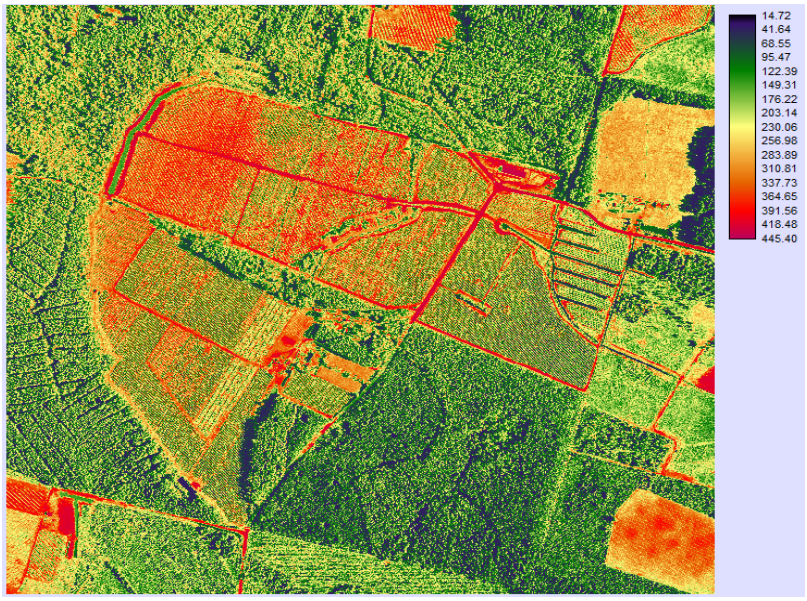

Figure 7: SAVI raster for AOI 3 Georgia site.

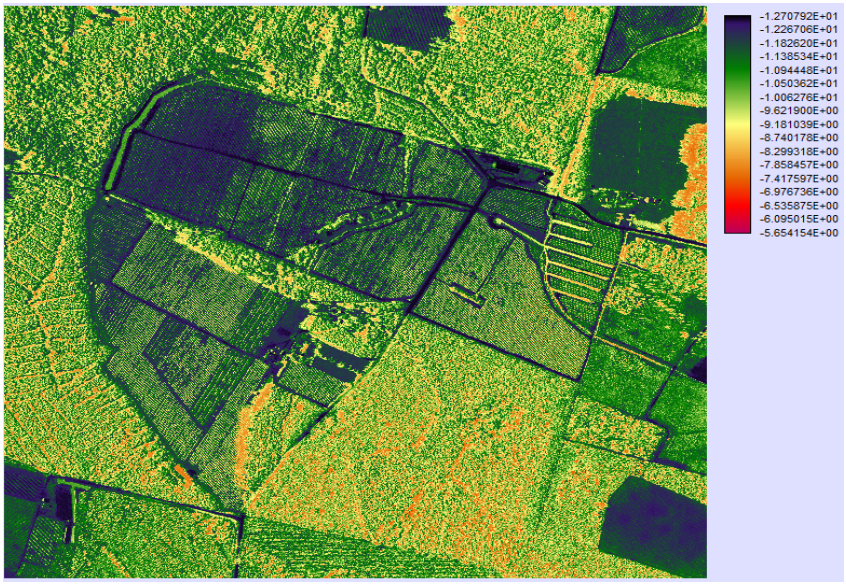

Figure 8: LAII raster for AOI 3 Georgia site

Forest plant speciation using OBIA technology for AOI 2 and AOI 3

Figures 9 a-f show results for step by step rule set developed for AOI 3 image segmentation. The rule set equations are inscribed inside the figures. It is to be noted, however, that any rule set developed for one study area may not be useful for another study area.

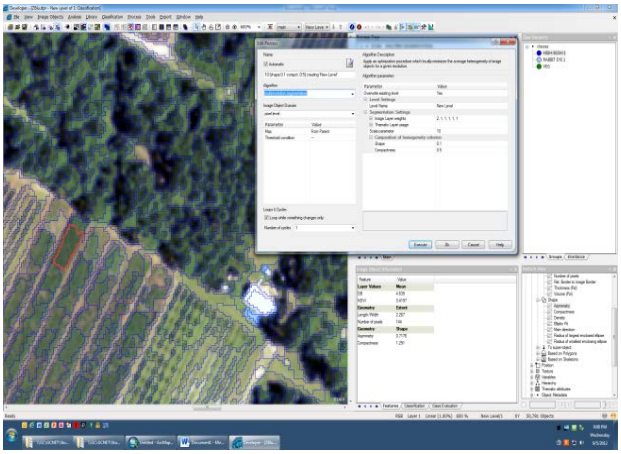

Fig 9a: Initial rule set and information for a selected object

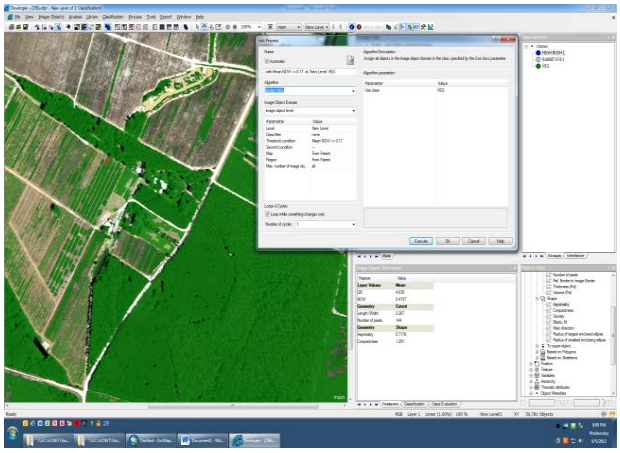

Fig 9b: Rule set for calculated NDVI

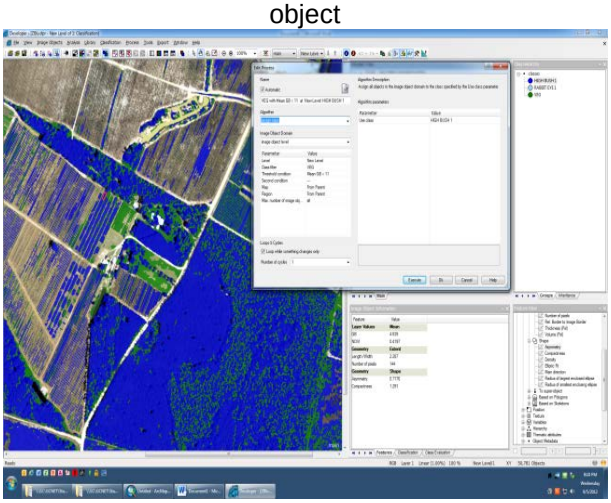

Fig 9c: Rule set for initial high bush classification with mixed result.

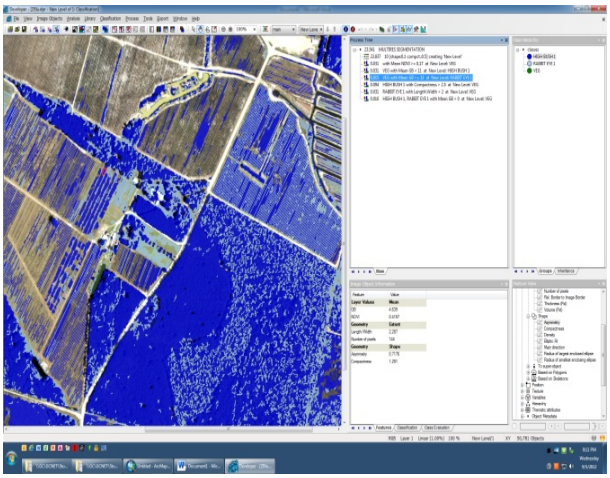

Fig 9d: Rule set for initial rabbit eye classification with mixed result.

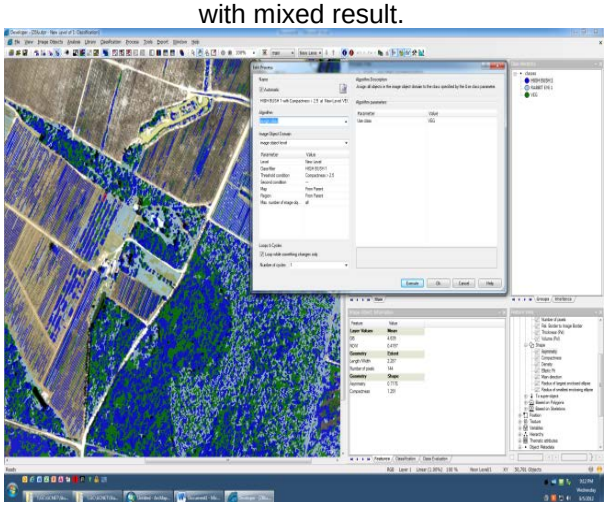

Fig 9e: Initial rule set for high bush classification with geometric attribute.

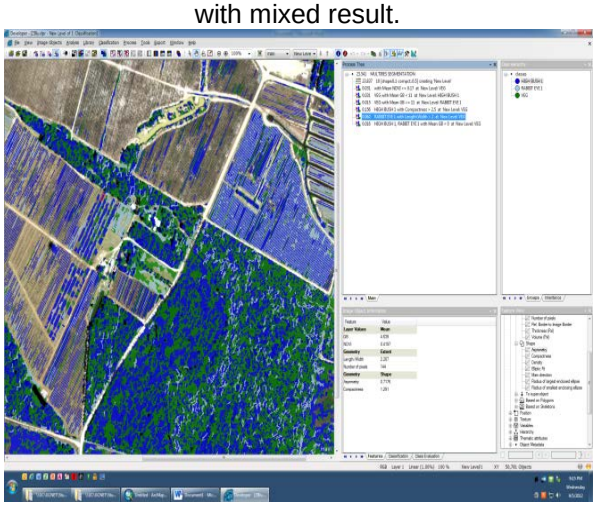

Fig 9f: Rule set for rabbit eye classification with geometric attribute

Figures 10 a-d show the rule sets developed using a step by step process with vegetation spectral characteristics, tree height, geometric shape of objects, and closeness to the thematic layers of the part Turkey Creek watershed. (AOI 2). The figures contain the rule sets that were developed in each process.

Fig 10a: Rule set to use tree height raster (nDSM) info for distinguishing orchards.

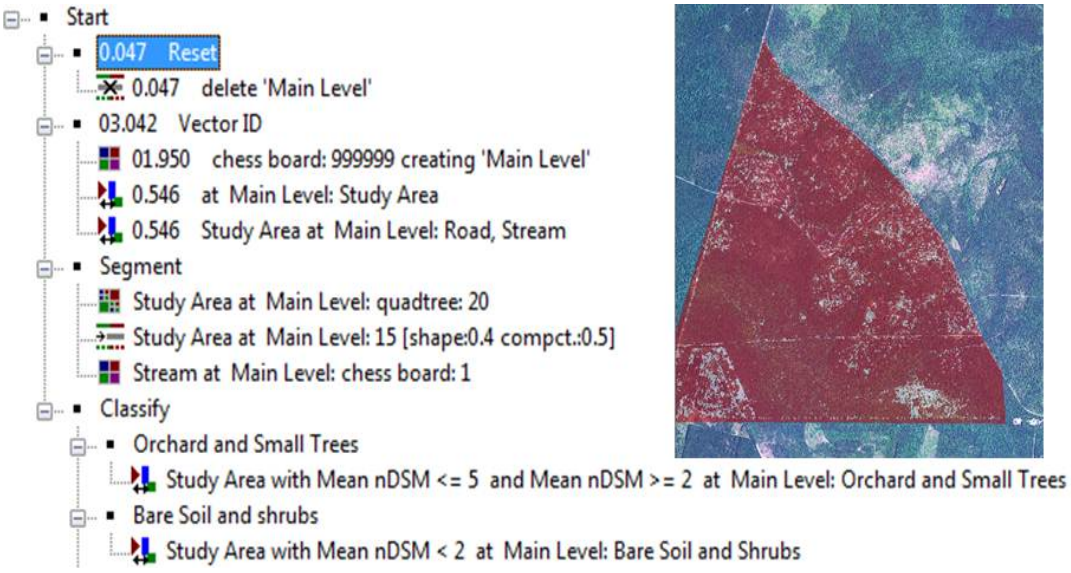

Fig 10b: Rule set to distinguish bare soil and shrubs using spectral characteristics.

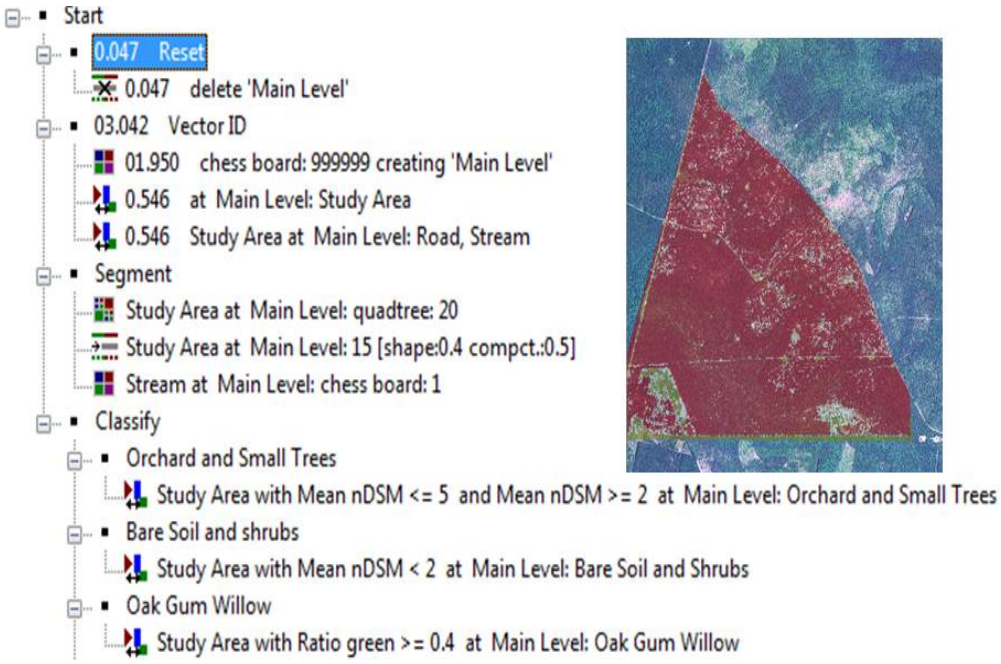

Fig 10c: Rule set to classify Oak/Gum/Willow trees using spectral & nDSM information.

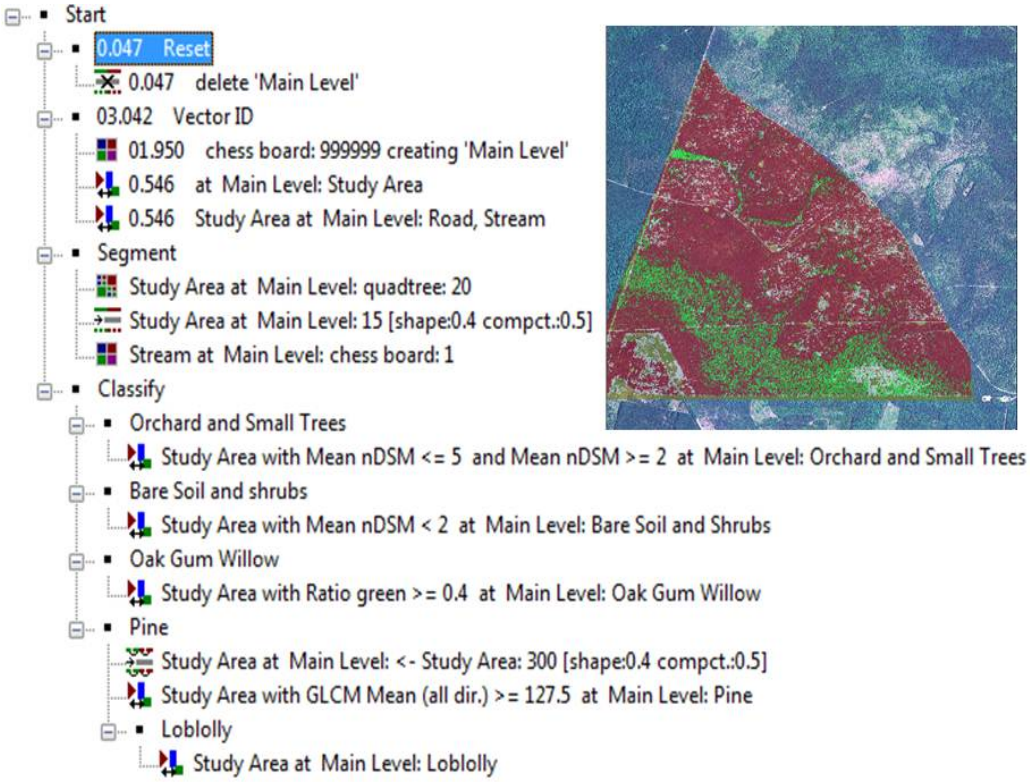

Fig 10d: Final rule set to distinguish loblolly pine from other vegetation using thematic layer proximity.

Figure 11 shows the final classified map of AOI 2 (part Turkey Creek forested watershed). The forest species such as oak/gum/willow, loblolly pine, other pine species, orchard, and small trees, bare soil and shrubs and other land-uses like roads and streams are distinguished in the part Turkey Creek watershed area and it was compared with the classification vector map (Figure 4) with satisfactory results. Figure 12 represents the final classification map of the Z-blu (AOI 3) orchard with three classes (Rabbit eye, high bush, forest vegetation). It compared very well with Figure 2b with a high accuracy. Proper groundtruthing for accuracy assessment has not been conducted at any site. It will be conducted soon and the OBIA classification models will be refined in future study. However, the land use classes obtained from the OBIA segmentation process were correlated with the forest cover classification map for AOI 2 (Figure 2a) site and Z-blu orchard management specification vector (Figure 2b) for AOI 3 and R^2 values of 0.84 and 0.88, respectively, were obtained.

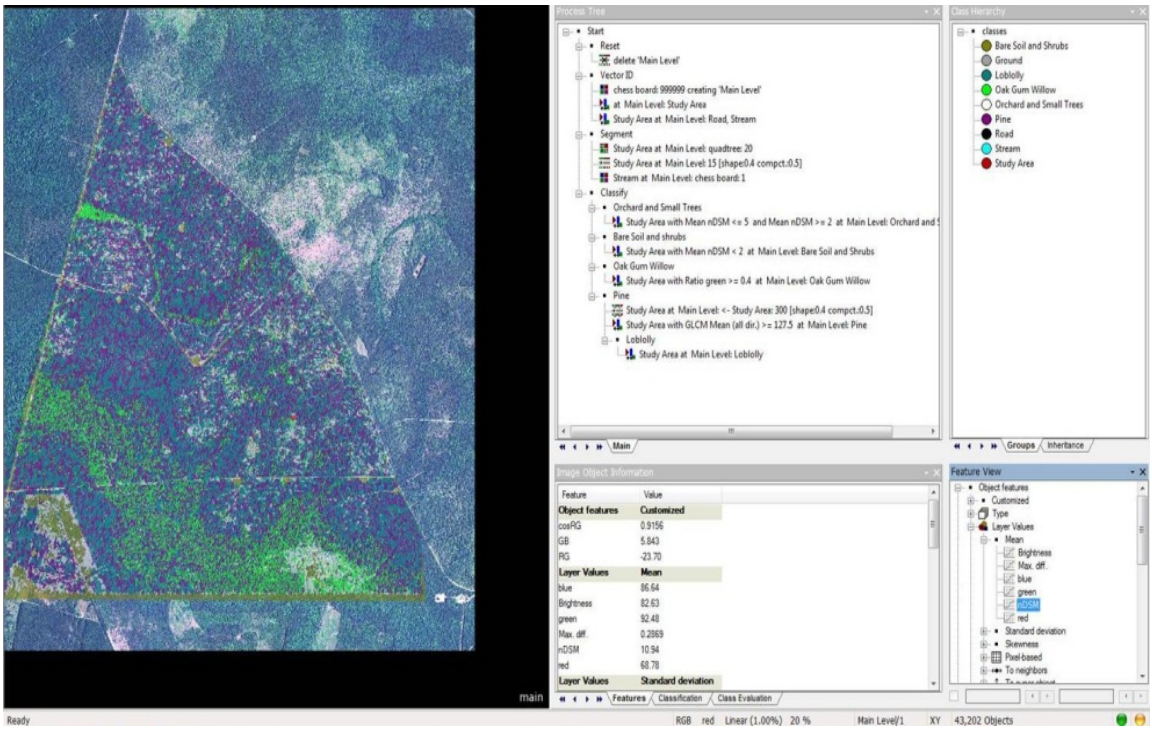

Fig 11: Final classified map of part Turkey Creek coastal forested watershed ((AOI 2) along with the rule sets.

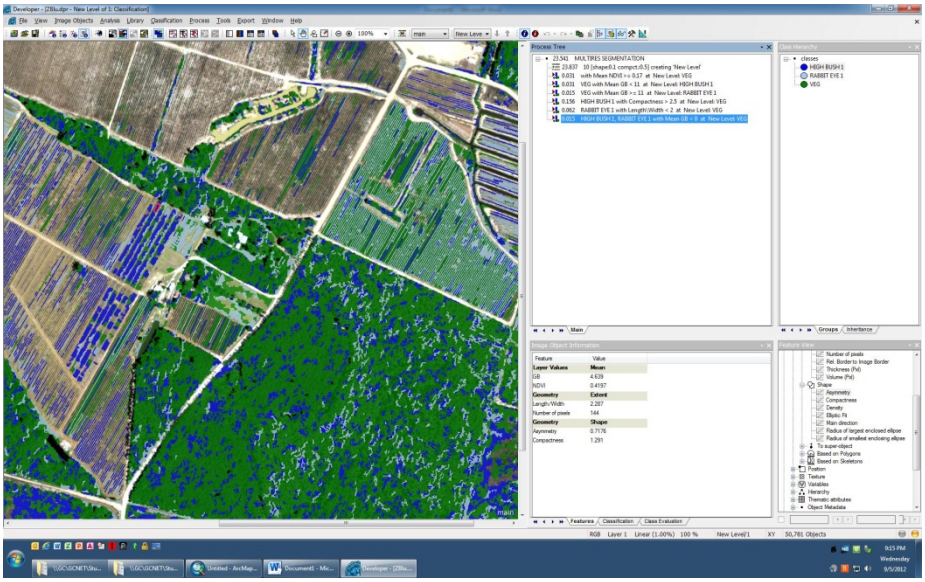

Fig 12: Final classified map of Z-Blu blueberry orchard (AOI 3) along with the rule sets.

Conclusions

The study confirms that plant canopy temperature, stomatal conductance, and LAI can be estimated reasonably well on spatial basis by using the correlation models developed with the data derived from analysis of spectral, textural, and other thematic attributes of remotely sensed imageries (LANDSAT ETM+7, NAIP, LiDAR) with corresponding field measurements. Rule sets based OBIA technique also performed well to classify different forest species at two coastal study sites with different vegetation although a thorough ground truthing and classification accuracy assessment is warranted. The result obtained from the LAI raster developed for the AOI 2 study site with pine and other hardwood mixed forest was also encouraging. When compared with the OBIA based classified image, a high visual correlation was observed for LAI and different plant species.

Acknowledgement

The authors would like to acknowledge the Weyerhaeuser Company and its staff for the historical data from the North Carolina site, the USDA Forest Service Francis Marion National Forest and its staff for the forest type distribution data from the South Carolina site, and the Z-Blu blueberry orchard farm staff from the Georgia site. The authors also would like to thank the

anonymous reviewers of this manuscript for their valuable comments and suggestions to improve the manuscript and Azal Amatya for a help with initial formatting of this manuscript.

References

Amatya and Skaggs. (2001). Hydrologic modeling of pine plantations on poorly drained soils. *Forest Science*, 47(1) 2001: 103-114.

Amatya, D., S.S. Panda, G. Cheschair, J. Nettles, T. Appleboom, and W. Skaggs, (2011). Evaluating evapotranspiration and stomatal conductance of matured pine using geospatial technology. American Geophysical Union Conference 2011, December 5-9, 2011.

Amatya, D.M. (1993). Hydrologic Modeling of Drained Forested Lands. Unpubl. *Ph.D. Dissertation*, North Carolina State University, Raleigh, NC.

Amatya, D.M. and M.K. Jha. (2011). Evaluating SWAT Model for a Low Gradient Forested Watershed in Coastal South Carolina. *Trans of the ASABE*, 54(6):2151-2163

Amatya, D.M., C. Trettin, S. Panda, and H. Ssegane. (2013). Application of LiDAR data for Hydrologic Assessments of Low-gradient Coastal Watershed Drainage Characteristics. J of Geographical Information System, 2013, 5, 171-195. Doi:10.4236/jgis.2013.52017 Published online April 2013 (https://www.scirp.org/journal/jgis).

Amatya, D.M., R.W. Skaggs and J.D. Gregory. (1996). Effects of Controlled Drainage on the Hydrology of a Drained Pine Plantation in the North Carolina Coastal Plains. *J. of Hydrology*, 181(1996), 211-232

Bastiaanssen, W. G. M., Menenti, M., Feddes, R. A., & Holtslag, A. A. M. (1998). A remote sensing surface energy balance algorithm for land (SEBAL). 1. Formulation. *Journal of hydrology*, *212*, 198-212.

Brauman, K.A., D.L. Freyberg, and G.C. Daily. (2012). Potential evapotranspiration from forest and pasture in the tropics: A Case study in Kona, Hawaii. J. of Hydrol., 440-441 (2012):52-61.

Burnett, C., Heurich, M., and Tiede, D. (2003). Exploring segmentation-based mapping of tree crowns: Experiences with Bavarian forest NP LiDAR/Digital Imagery Dataset. Presented in the International Conference & Workshop, ScanLaser 2003., Umea, Sweden, September 2-4, 2003.

Carter, G. A. (1998). Reflectance wavebands and indices for remote estimation of photosynthesis and stomatal conductance in pine canopies. *Remote Sensing of Environment*, *63*(1), 61-72.

Coonrod, J. and D. McDonnell. (2000). Using Remote Sensing and GIS to Compute Evapotranspiration in the Rio Grande Bosque. Proceedings of the ESRI User Conference 2000, San Diego, CA. Retrieved from http://proceedings.esri.com/library/userconf%20/proc01/professional/papers/pap487/p487.htm.

Curran, P. J. (1980), Multispectral remote sensing of vegetation amount, Prog. Phys. Geogr., 4, 315–341.

Fisher, J.B., K.P. Tu, and D.D. Baldocchi. (2008). Global estimates of the land-atmosphere water flux based on monthly AVHRR and ISLSCP-II data, validated at 16 FLUXNET sites. Remote Sensing of Environment, Vol. 112, Issue 3, March 2008, 901-919.

Goel, N. S., and W. Qin (1994). Influences of canopy architecture on relationships between various vegetation indices and LAI and FPAR: A computer simulation, Remote Sens. Rev., 10(4), 309–347.

Hafeez, M.M., Y. Chemin, V.D. Geisen, N., and Bouman, B.A.M. (2002). Field evapotranspiration estimation in Central Luzon, Philippines using different sensors: LandSat 7ETM+, Terra Modis, and Aster. In Proc., Symposium on Geospatial Theory, Processing, and Applications, Ottawa, Canada, 2002, 7 p.

Haley, E.B. (2007). Field measurements and hydrologic modeling of the Turkey Creek watershed, South Carolina. M.S. Thesis, Graduate School of the College of Charleston, 2007.

Huete, A. R. (1988). A soil adjusted vegetation index (SAVI). Remote Sensing Environment, 25: 295-309.

Hwang, T., L. Band, and T.C. Hales. (2009). Ecosystem processes at the watershed scale: Extending optimality theory from plot to catchment. Water Res. Res., Vol. 45, W11425, doi:10.1029/2009WR007775, 2009, 20 p.Lilles and and Keifer, 1994, *Remote Sensing and Image Interpretation*, 3rd. ed., John Wiley &Sons, Inc., page 376.

Justice, C. O., Vermote, E. , Townshend, J. R. G. , DeFries, R. , Roy, D. P. , Hall, D. K. , Salomonson, V. V. , Privette, J. L. , Riggs, G. , Strahler, A. , Lucht, W. , Myneni, R. B. , Knyazikhin, Y. , Running, S. W. , Nemani, R. R. , Zhengming W. , Huete, A. R. , Van Leeuwen, W. , Wolfe, R. E. , Giglio, L. , Muller, J.-P. , Lewis, P. , Barnsley, M. J. (1998). The Moderate Resolution Imaging

Spectroradiometer (MODIS): Land remote sensing for global change research, IEEE Trans. Geosci. Remote Sens., 36(4), 1228– 1249.

le Maire, G., C. Franc¸ois, K. Soudani, H. Davi, V. Le Dantec, B. Saugier, and E. Dufreˆne (2006). Forest leaf area index determination: A multiyear satellite-independent method based on within-stand normalized difference vegetation index spatial variability, J. Geophys. Res., 111, G02027, doi:10.1029/2005JG000122.

Lee, J. G. (1994). *Counterspace Operations for Information Dominance*. Air univ maxwell afb al school of advanced airpower studies.

Lillesand and Keifer, (1994). *Remote Sensing and Image Interpretation*, 3rd. ed., John Wiley &Sons, Inc., page 376.

McCarthy, E.J., R.W. Skaggs, and P. Farnum. (1991). Experimental determination of the hydrologic components of a drained forest watershed. *Trans. Amer. Soc. Agr. Eng*., 34(5):2031-2039.

Moran, M. S., Clarke, T. R., Inoue, Y., & Vidal, A. (1994). Estimating crop water deficit using the relation between surface-air temperature and spectral vegetation index. *Remote sensing of environment*, *49*(3), 246-263.

Narasimhan, B., R. Srinivasan, and A.D. Whittaker. (2003). Estimation of Potential Evapotranspiration from NOAA-AVHRR Satellite. 2003. Applied Engrg. In Agric., ASAE, 19(3):309-318.

North, P. R. J. (2002). Estimation of fAPAR, LAI, and vegetation fractional cover from ATSR-2 imagery, Remote Sens. Environ., 80, 114–121.

Nouri, H., Beecham, S., Kazemi, F., & Hassanli, A. M. (2012). A review of ET measurement techniques for estimating the water requirements of urban landscape vegetation. *Urban Water Journal*, (ahead-of-print), 1-13.

Olioso, A., Chauki, H., Courault, D., & Wigneron, J. P. (1999). Estimation of evapotranspiration and photosynthesis by assimilation of remote sensing data into SVAT models. *Remote Sensing of Environment*, *68*(3), 341-356.

Panda, S.S., J. Nolan, D. Amatya, K. Dalton, R.M. Jackson, H. Ssegane, and G. Chescheir. (2012). Stomatal conductance and leaf area index estimation using remotely sensed information and forest speciation. Presented in the 3rd International Conference on Forests and Water in

Changing Environment 2012, Fukuoka, Japan. September 18 –20, 2012.

Panda, S.S., P. Peters, R. Harris, and R.J. Skarda, (2011). Remote measurement of potential water loss through evapo-transpiration of kudzu during the growing season. National Water Conference 2011, January 31-February 1, 2011, Washington, DC.

Pearcy, R. W., Schulze, E. D., & Zimmermann, R. (1989). Measurement of transpiration and leaf conductance. In *Plant physiological ecology* (pp. 137-160). Springer Netherlands.

Provoost, S.; Van Til, M.; Deronde, B.; Knotters, A. (2005). Remote sensing of coastal vegetation in the Netherlands and Belgium, *in*: Herrier, J.-L. *et al.* (Ed.) (2005). *Proceedings 'Dunes and Estuaries 2005': International Conference on nature restoration practices in European coastal habitats, Koksijde, Belgium 19-23 September 2005. VLIZ Special Publication,* 19: pp. 139-149.

Rouse, J. W., R. H. Haas, J. A. Schell, and D. W. Deering (1973). Monitoring vegetation systems in the great plains with ERTS, in Third ERTS Symposium, SP-351, pp. 309– 317, NASA, Washington, D. C.

Sack, L., & Scoffoni, C. (2012). Measurement of Leaf Hydraulic Conductance and Stomatal Conductance and Their Responses to Irradiance and Dehydration Using the Evaporative Flux Method (EFM). *Journal of visualized experiments: JoVE*, (70).

Sampson, D.A., D.M. Amatya, C.D. Blanton, and R.W. Skaggs. (2011). Leaf area index (LAI) of Loblolly pine and Emergent Vegetation Following a Harvest. *Trans. Of the ASABE*, 54(6):2057-2066.

Schultz, G. A. and Engman, E. T. (2000). Remote Sensing in Hydrology and Water Management.Springer, Heidelberg, Germany.

Seetha, M., MuraliKrishna, I.V., and Deekshatulu, B.L. (2014). Comparison of advanced techniques of image classification. GIS Development. http://www.gisdevelopment.net/proceedings/mapworldforum/rsp/MWF_Remote_78.pdf. Accessed on February 3, 2014.

Senay, G.B., S. Bohms, R.K. Singh, P.H. Gowda, N.M. Velpuri, H. Alemu, and J.P. Verdin. (2013). Operational Evapotranspiration Mapping Using Remote Sensing and Weather Datasets: A New Parameterization for the SSEB Approach. J. Amer. Water Resou. Assoc. (JAWRA), 1-15, DOI:10.1111/jawr.12057

Ssegane, H., D.M. Amatya, A. Muwamba, G.M. Chescheir, and J.E. Nettles. (2014). Hydrologic Calibration of Watersheds with Switchgrass and Its Intercropping on Pine Forest in Coastal North Carolina. Draft manuscript in review.

Sun, G., K. Alstad, J. Chen, S. Chen, C. R. Ford, G. Lin, N. Lu, S. G. McNulty, A. Noormets, J. M. Vose, B. Wilske, M. Zeppel, Y. Zhang, and Z. Zhang. (2011). A general predictive model for estimating monthly ecosystem evapotranspiration. *Ecohydrol*. 4:245-255, doi:10.1002/eco.194.

Tian, S., M.A. Youssef, R.W. Skaggs, D.M. Amatya, and G.M. Chescheir. (2012). DRAINMOD-FOREST: Integrated modeling of Hydrology, Soil Carbon, and Nitrogen Dynamics, and Plant Growth for Drained Forest. *Journal of Environmental Quality* 41:764-782 (2012).

Turner, D. P., W. B. Cohen, R. E. Kennedy, K. S. Fassnacht, and J. M. Briggs (1999). Relationships between leaf area index and Landsat TM spectral vegetation indices across three temperate zone sites, Remote Sens. Environ., 70, 52– 68.

Viessman, W. and Lewis, G. L. (2004). *Introduction to Hydrology*. Upper Saddle River, NJ: Prentice Hall

Walthall, C., W. Dulaney, M. Anderson, J. Norman, H. Fang, and S. Liang (2004). A comparison of empirical and neural network approaches for estimating corn and soybean leaf area index from Landsat ETM+ imagery, Remote Sens. Environ., 92, 465– 474.

Wang, L., & Qu, J. J. (2009). Satellite remote sensing applications for surface soil moisture monitoring: A review. *Frontiers of Earth Science in China*, *3*(2), 237-247.

Willaert, L., Samson, R., Provoost, S., Verbeke, L., Lemeur, R., Meuleman, K., & De Wulf, R. (2005). LAI determination in dune vegetation: a comparison of different techniques. *VLIZ Special Publication*, *19*.